organics

MDPI

Article

On the Mechanism of the Synthesis of Nitrofunctionalised Δ^2-Pyrazolines via [3+2] Cycloaddition Reactions between α-EWG-Activated Nitroethenes and Nitrylimine TAC Systems

Agnieszka Fryźlewicz, Aleksandra Olszewska, Karolina Zawadzińska, Przemysław Woliński, Karolina Kula, Agnieszka Kącka-Zych, Agnieszka Łapczuk-Krygier and Radomir Jasiński *

Department of Organic Chemistry and Technology, Cracow University of Technology, Warszawska 24, 31-155 Cracow, Poland; aga.fryzlewicz@poczta.fm (A.F.); aleksandra.o1@o2.pl (A.O.); karolina.zawadzinska@doktorant.pk.edu.pl (K.Z.); przemyslaw.wolinski@pk.edu.pl (P.W.); karolina.kula@pk.edu.pl (K.K.); agnieszka.kacka-zych@pk.edu.pl (A.K.-Z.); agnieszka.lapczuk-krygier@pk.edu.pl (A.Ł.-K.)

* Correspondence: radomir.jasinski@pk.edu.pl

Abstract: We investigated the reactivity of different substituted nitrylimine-type three atom components (TACs) in [3+2] cycloaddition (32CAs) reactions with electrophilically activated nitroethenes within molecular electron density theory (MEDT). In parallel research, the molecular mechanism of the considered transformation was examined through analysis of all possible reaction channels and full optimization of all critical structures. In particular, the existence of zwitterionic intermediates on reaction paths was verified. On the basis of the bonding evolution theory (BET), the mechanism of the 32CA reaction between C,N-diphenylnitrylimine and (E)-2-phenyl-1-cyano-1-nitroethene should be treated as a one-step two-stage mechanism.

Keywords: [3+2] cycloaddition; nitrilimine; nitroalkene; Δ^2-pyrazoline; molecular electron density theory (MEDT)

check for updates

Citation: Fryźlewicz, A.; Olszewska, A.; Zawadzińska, K.; Woliński, P.; Kula, K.; Kącka-Zych, A.; Łapczuk-Krygier, A.; Jasiński, R. On the Mechanism of the Synthesis of Nitrofunctionalised Δ^2-Pyrazolines via [3+2] Cycloaddition Reactions between α-EWG-Activated Nitroethenes and Nitrylimine TAC Systems. *Organics* **2022**, *3*, 59–76. https://doi.org/10.3390/org3010004

Academic Editor: David StC Black

Received: 16 December 2021
Accepted: 7 February 2022
Published: 1 March 2022

1. Introduction

This work is a continuation of our comprehensive, experimental, and theoretical study regarding the synthesis and reactivity of (E)-2-aryl-1-cyano-1-nitroethenes (ACN). Some examples of this group of conjugated nitroalkenes have been known since the second half of the 20th century [1,2]. In recent years, similar-type compounds have been synthetized [3,4]. Unfortunately, knowledge of their chemical properties is still limited. Recently, we detected a series of interesting chemical properties of ACNs regarding their participation in cycloaddition processes. For example, despite the high reactivity of the shielded reaction sites, ACNs react rapidly with cyclopentadiene even at r.t., yielding mixtures of respective endo-nitro and exo-nitro cycloadducts [5] (Scheme 1). In similar reactions involving the mixture of methylcyclopentadienes, of which many are possible, stereoisomeric products are formed [6]. In contrast, less sterically crowded 2-aryl-1-nitroethenes react with cyclopentadiene at temperatures up to 80 °C [7].

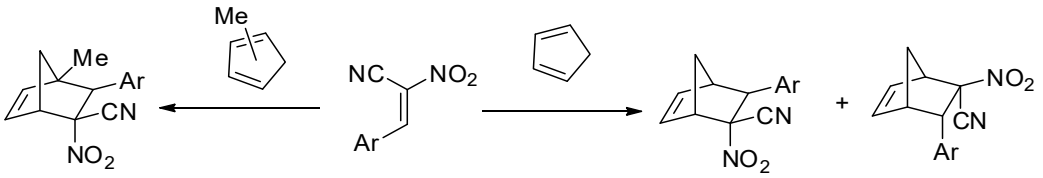

Scheme 1. Cycloaddition reactions of conjugated dienes with CNAs.

[3+2] cycloaddition (32CA) reactions of ACNs and N-methylazomethine ylide proceed under mild conditions and produce nitropyrrolidines [8]. In contrast, in analogous 32CAs involving diazafluorene, zwitterionic acyclic adducts were formed in the first reaction step. These zwitterions converted spontaneously under the reaction conditions into azine molecular systems [9]. At the same time, other nitroalkenes characterized by similar electrophilicity as ACNs reacted with diazafluorene to produce Δ^1-nitropyrazolines (Scheme 2).

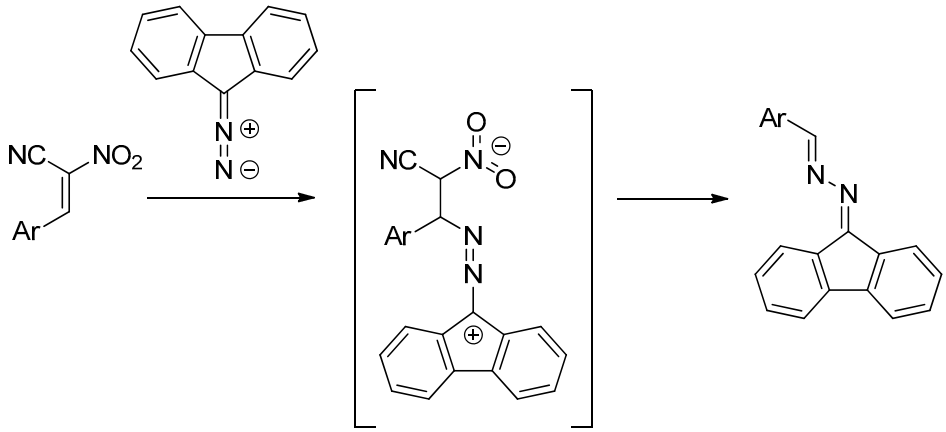

Scheme 2. The zwitterionic intermediate in reaction of diazafluorene and ACNs.

Non-catalyzed 32CA reactions between ACNs and nitrile N-oxides proceed unexpectedly with the participation of a nitrile bond, instead of resulting in the expected >C=C< moiety of nitroalkene [10] (Scheme 3). There are evidently rare cases of 32CAs in the CN bond, which is generally recognized as inactive in the 32CA processes.

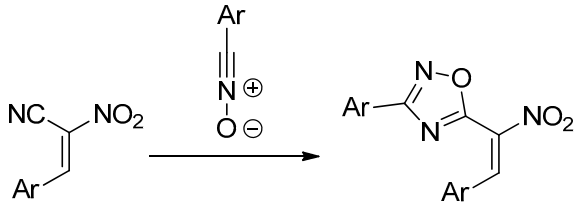

Scheme 3. 32CAs converting to a nitrile CN bond of ACNs.

There is currently no published work regarding the participation of ACNs in 32CA processes involving nitrylimine TAC systems. Our work initiates comprehensive research in this area. We aim to shed light on the selectivity and molecular mechanism of model processes involving different substituted diarylnitrylimines (DNI) and ACNs. This analysis will be help to guide further experimental study in the presented area.

2. Computational Details

The global reactivity descriptors of the addends, namely electronic potential μ, chemical hardness η, global electrophilicity ω and global nucleophilicity N, were approximated in pursuance of the equations defined on the basis of conceptual density functional theory (CDFT) according to the equations recommended by Parr [11] and Domingo [12,13]. In the calculation we used the correlation-exchange functional B3LYP together with the basic level set of 6-31G(d) in the gas phase [12–15].

The electronic chemical potentials (μ) and chemical hardness (η) were evaluated in terms of one-electron energies of FMO (E_{HOMO} and E_{LUMO}) using the following equations [11–16]:

$$\mu \approx (E_{HOMO} + E_{LUMO})/2 \quad (1)$$

$$\eta \approx E_{HOMO} - E_{LUMO} \quad (2)$$

where E_{HOMO} and E_{LUMO} may be approached in terms of the one-electron energies of the frontier MOs respectively HOMO and LUMO. Next, values of μ and η were then used to calculate a global electrophilicity (ω) according to the formula [12,13]:

$$\Omega = \mu^2/\eta \quad (3)$$

The global nucleophilicity (N) can be presented as follow [13]:

$$N = E_{HOMO} - E_{HOMO\ (TCE)} \quad (4)$$

where $E_{HOMO\ (TCE)}$ is the HOMO energy for tetracyanoethylene (TCE); is the reference, because it presents the lowest HOMO ($E_{HOMO\ (TCE)}$ = −9.368 eV).

The local electrophilicity (ω_k) and the local nucleophilicity (N_k) concentrated on atom k was calculated based on global properties and the Parr function (P_k^+ or P_k^-), according to the formulas [17]:

$$\omega_k = P^+_k \cdot \omega \quad (5)$$

$$N_k = P^-_k \cdot N \quad (6)$$

For localization of the transition states (TSs) the wb97xd/6-311+g(d) level of theory was applied [18]. All transition states were verified by diagonalization of the Hessian matrix and by analysis of the intrinsic reaction coordinates (IRC). For the simulation of solvents effect, the polarizable continuum model (PCM) [19] was used. Calculations of all critical structures were performed for the temperature T = 298 K and pressure p = 1 atm. Global electron density transfer (GEDT) [20] was calculated according to the formula:

$$GEDT = -\Sigma q_A \quad (7)$$

where q_A is the net Mulliken charge and the sum takes over all the atoms of nitroalkene.

Indexes of σ-bonds development (I) were calculated according to formula [21]:

$$I_{A\text{-}B} = 1 - [(r^{TS}{}_{A\text{-}B} - r^{P}{}_{A\text{-}B})/r^{P}{}_{A\text{-}B}) \quad (8)$$

where $r^{TS}{}_{A\text{-}B}$ is the distance between the reaction centers A and B at the TS and $r^{P}{}_{A\text{-}B}$ is the same distance at the corresponding product.

The electron localization function (ELF) [22–24] and BET [25] studies were conducted according to well-known procedure using the TopMod [26] program. This approach to explain the molecular mechanism of various classes of compounds has been the subject of many studies [10,27–34].

3. Results and Discussion

Theoretically possible, regioisomeric channels of the analyzed reactions are presented on Scheme 4. In particular, according to competitive reaction channels, 1,3,5-triaryl-4-cyano-4-nitro-Δ^2-pyrazolines **3** and/or 1,3,4-triaryl-5-cyano-5-nitro-Δ^2-pyrazolines **4** can be formed in the consequence of interactions between addends. Firstly, we decide to lead an exploration of the nature of these interactions.

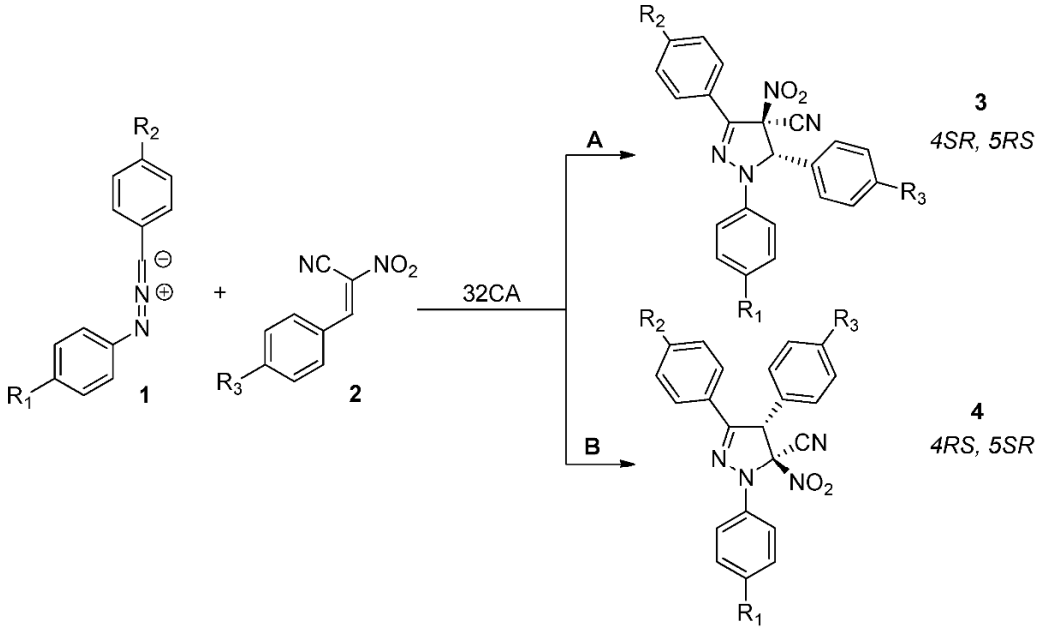

Reaction	Nitrylimine	Nitroalkene	R_1	R_2	R_3	Products	
1	**1a**	**2a**	H	H	H	**3aa**	**4aa**
2	**1b**	**2a**	NH_2	H	H	**3ba**	**4ba**
3	**1c**	**2a**	NO_2	H	H	**3ca**	**4ca**
4	**1d**	**2a**	H	NH_2	H	**3da**	**4da**
5	**1e**	**2a**	H	NO_2	H	**3ea**	**4ea**
6	**1a**	**2b**	H	H	NH_2	**3ab**	**4ab**
7	**1a**	**2c**	H	H	NO_2	**3ac**	**4ac**

Scheme 4. Theoretically possible channels of [3+2] cycloadditions between diarylnitrylimines **1a–e** and ACNs **2a–c**.

3.1. Nature of Intermolecular Interactions of Addents According to the Analysis Based on the CDFT Reactivity Indices of Reagents

3.1.1. Global Reactivity

The Conceptual Density Functional Theory (CDFT) should be considered as a strong implement that helps comprehension the reactivity of components in polar processes such as cycloaddition. All of indices was determined via calculations based on B3LYP/6-31G(d) theory level in the gas phase. It is very useful for estimate electrophilicity and nucleophilicity of the reagents [35–37]. Due to this, such indices as global reactivity indices: electronic chemical potential μ, chemical hardness η, global electrophilicity ω, global nucleophilicity N were determined and given in Table 1.

Table 1. Global electronic properties (electronic chemical potential μ, chemical hardness η, global electrophilicity ω, and nucleophilicity N; all in eV) for the studied addends.

	μ	η	ω	N
1a	–3.37	3.78	1.50	3.86
1b	–2.99	3.47	1.29	4.40
1c	–3.95	3.40	2.29	3.47
1d	–3.02	3.97	1.15	4.11
1e	–3.92	3.25	2.36	3.58
2a	–5.28	4.07	3.42	1.81
2b	–4.51	3.48	2.92	2.87
2c	–5.98	4.00	4.47	1.14

Analysis of the electronic chemical potential μ, can define the direction of the electron density flux between reagents in determined path of reaction. In case of the model reaction between nitrylimine **1a** and nitroethene **2a**, the electronic chemical potential μ [35,36] of **1a**, −3.37 eV, is significantly higher than this of **2a**, −5.28 eV, (Table 1). That means, in a course of model reaction **1a** with **2a**, the electron density flux will take place from nitrylimine **1a** to nitroethene **2a**. Similar results can be observed for the other reagents, as long as all the nitrylimine components **1b**–**e** can be characterized by substantially higher value of electronic chemical potential than nitroethanes **2b**–**c** (Table 1).

Calculated index of electrophilicity [35,36] ω of C,N-diphenylnitrylimine (**1a**) is 1.50 eV. In turn, the calculated index of nucleophilicity [13] N for this compound is 3.86 eV (Table 1). These values give the conclusion that model nitrylimine **1a** acts similar to moderate electrophile and strong nucleophile in a polar reaction.

Introduction of electron-donating (ED) $–NH_2$ group at *para* position of the phenyl ring in nitrylimine **1a** slightly reduces the electrophilicity ω index of **1b** and **1d**, 1.15 and 1.29 eV, respectively, slightly increases the nucleophilicity N index to 4.40 eV (**1b**) and 4.11 eV (**1d**) (Table 1). In a consequence, both C-phenyl-N-(4-aminophenyl)-nitrylimine (**1b**) and C-(4-aminophenyl)-N-phenylnitrylimine (**1d**) can be considered as a moderate electrophiles and also strong nucleophiles.

On the other hand, the presence of electron-withdrawing (EWG) $–NO_2$ group at *para* position of the phenyl ring in nitrylimine **1a** significantly increases the electrophilicity ω index of **1c** and **1e**, respectively, 2.29 and 2.36 eV, and also slightly reduces the nucleophilicity N index to 3.47 eV (**1c**) and 3.58 eV (**1e**) (Table 1). Consequently, C-phenyl-N-(4-nitrophenyl)-nitrylimine (**1c**) and C-(4-nitrophenyl)-N-phenylnitrylimine (**1e**) can be classified both as a strong electrophiles and strong nucleophiles. Simultaneously, these nitrylimines will behave as ambiphilic species [38,39].

In turn, calculated phenyl index of nucleophilicity N for this compound is 2.87 eV (Table 1). These values provide the conclusion that model nitroalkene **2a** acts similar to strong electrophile and also moderate nucleophile in a polar reaction.

The presence of both ED group such as $–NH_2$ or and EWG group such as $–NO_2$ in at *para* position of the phenyl ring in nitroalkene **2a** significantly changes global electronic properties. Especially, it increases the electrophilicity ω index to 3.42 (**2b**) and 4.47 eV (**2c**) and slightly reduces nucleophilicity N index to 1.81 (**2b**) and 1.14 eV (**2c**) (Table 1). Therefore, both of (E)-2-(4-aminophenyl)-1-cyano-1-nitroethenes (**2b**) and (E)-2-(4-nitrophenyl)-1-cyano-1-nitroethenes (**2c**) can be classified as a marginal nucleophile but remains as a strong electrophile.

Polar cycloaddition reactions require the participation of good electrophiles and good nucleophiles. CDFT reactivity indices show that all of analyzed (E)-2-aryl-1-cyano-1-nitroethenes **2a**–**c** can be classified as evidently strong electrophiles. In turn, the simplest C,N-diphenylnitrylimine (**1a**) and *para* amino analogues of diarylnitrylimines **1b** and **1d** can be classified as moderate electrophiles. It follows that, the difference in electrophilicity Δω index between components NIs and CNAs is significant (Δω > 1 eV) (Table 1). Therefore, it is expected, that the 32CA reaction of nitrylimines **1a**, **1b** and **1d** with nitroethenes **2a**–**c** will have a polar character. In turn, nitro substituted diarylnitrylimines **1c** and **1e** can be classified as strong electrophiles. These components have an evidently higher electrophilicity ω index than nitrylimines **1a**, **1b**, **1d** (Table 1). It causes, that the difference in electrophilicity Δω between components *para* nitro NIs (**1c**, **1e**) and CNAs (**2a**–**c**) has been significantly lower compared to the previous 32CAs (**1a**, **1b**, **1d** + **2a**–**c**) (Δω < 1 eV) (Table 1). It follows that, the 32CA reaction of nitrylimines **1c** and **1e** with nitroethenes **2a**–**c** will not have a polar character [13,16].

Very recently, organic reactions have been classified as forward electron density flux (FEDF) and reverse electron density flux (REDF) reactions, depending on the direction of the flux of the electron density [38,40]. Non-polar reactions are classified as null electron density flux (NEDF) reactions [38,41]. Thus, the reactions involving nucleophilic nitrylimines **1a**, **1b** and **1d** and electrophilic nitroalkenes **2a**–**c** are classified as FEDF in agreement with the

CDFT analysis. On the other hand, the non-polar 32CA reactions of **1c** or **1e** with all of the nitrylimine components **1a**–**e** should be classified as NEDF.

3.1.2. Local Reactivity

The regioselectivity of polar processes of non-symmetric reagents can be specified through interaction between the most electrophilic center of the electrophile and the most nucleophilic ones of the nucleophile. For this purpose, electrophilic P_k^+ and nucleophilic P_k^- Parr functions, derived from the changes of spin electron density reached via the GEDT process from the nucleophile to the electrophile, can be used as a powerful tool in the study of the local reactivity [42–44]. According to the nucleophilic P_k^- Parr functions of nitrylimine components **1a**,**c**,**e** and the electrophilic P_k^+ Parr functions of nitroethanes **2a**–**c** in order to characterize the most nucleophilic and electrophilic centers of the species involved in this polar 32CA reaction were analyzed (Figure 1).

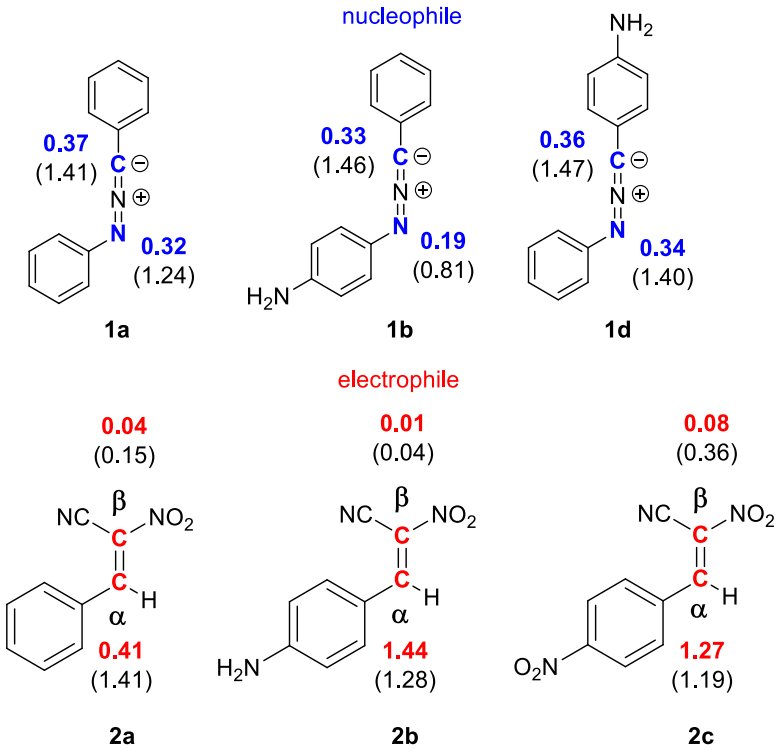

Figure 1. The local electronic properties of nitrylimines **1a**,**c**,**e** and nitroethanes **2a**–**c**. The nucleophilic P_k^- given in blue and the electrophilic P_k^+ given in red; the indexes of local nucleophilicity N_k and local electrophilicity ω_k given in brackets.

Analysis of the electrophilic P_k^+ Parr functions of (E)-2-phenyl-1-cyano-1-nitroethenes (**2a**) indicates that the most electrophilic center is situated on carbon atom ***α***, P_k^+ = 1.41 eV (Figure 1). The presence of amino or nitro group at *para* position of the phenyl ring of nitroethenes **2b** and **2c** does not cause significant changes in local reactivity. It means that for nitroethenes **2b** and **2c** the most electrophilic center is also located in atom ***α*** of carbon, P_k^+ = 1.44 eV (**2b**) and 1.27 eV (**2c**), respectively (Figure 1). It implies that center will react with the most nucleophilic ***α*** center of nitrylimines **1a**,**c**,**e**.

On the other hand, the analysis of the nucleophilic P_k^- Parr functions of the C,N-diphenylnitrylimine (**1a**) indicates that the carbon atom of –N=N=C– fragment constitutes the most nucleophilic center at molecule, presenting the maximum values at P_k^- = 0.32 eV (Figure 1). Same as in the previous example the presence of amino group at *para* position of the benzene ring for nitroethenes **2c** and **2e** does not significantly change the values of local reactivities. Therefore, nitrylimines **2c** and **2e** show a similar reactivity when compared

with C,N-diphenylnitrylimine (**1a**) and presenting the maximum values at $P_k^- = 0.33$ (**2c**) and 0.36 (**2e**) eV, respectively (Figure 1).

Summarizing, according to CDFT theory [12,14] the polar reactions of nitrylimines **1a**,**c**,**e** with nitroalkenes **2a**–**c** will be realized through the interaction of α atom of carbon for **1a**,**c**,**e** with the carbon atom of –N=N=C– fragment for **2a**–**c**. Therefore, the more preferred reaction channel for analyzed [3+2] cycloaddition reactions are forming 5-nitro-substituted Δ^2-isoxazolines **4a**,**c**,**e** according to path B. The regioselectivity of 32CA between nitrylimines **1a**,**c**,**e** and nitroalkenes **2a**–**c** cannot be determined using similar approach due to the non-polar nature of these processes [45].

3.2. Reaction Profiles

The mechanistic study regarding the title reactions we initiated from the exploration of the model process involving parent nitrylimine **1a** and parent CNA **2a**. It was found, that in toluene solution, the nature of energy profiles of both considered reaction channels are qualitatively similar (Figure 2). In particular, between valleys of individual reagents and products, two critical points were localized. These are connected with the existence of pre-reaction molecular complexes (**MC**) as well as transition states (**TS**). The first transformation of the reaction system is a formation of **MC**. This stage is characterized by reduction of the enthalpy of the reaction system about 11–12 kcal/mol (Table 2). However, the entropy factors do not determine the possibility of the existence of **MC**s as stable intermediates ($\Delta G > 0$ kcal/mol). Within **MC**s, addends are oriented relatively, for the achieving maximally good coulombic interactions between substructures (Table 3, Figure 3). These are not a charge-transfer complexes, which was confirmed by GEDT analysis [20]. Within MCs, reaction centers are oriented for the fashion, which determine further, positive interactions between substructures. Key interatomic distances (Tables 4 and 5) are characterized by values which are beyond of the typical range for formed sigma-bonds in transition states. The further conversion of **MC**s, lead on both considered paths to area of the existence of **TS**s. This requires an overcome of the energetical barrier about 8kcal/mol. It should be mentioned, that both considered paths should be permitted, as allowed from the kinetic point of view. Next, small difference between energies of the activation suggest rather low reaction regioselectivity. Within **TS**s, great amount of the charge transfer between substructures are observed (0.67e and 0.39e for **TSA** and **TSB**, respectively). This confirms expected previously, polar nature of considered cycloadditions. Next, in the framework of **TS**, the key interatomic distances are reduced substantially, in the comparison for analogous distances within **MC**s. The formation of new sigma-bonds proceeds evidently according to the asynchronous manner (Tables 4 and 5). This is typical for polar 32Cas processes involving unsymmetrical substituted components. The asynchronicity of TSs are however not sufficient for the extort the stepwise mechanism of the cycloaddition. The IRC analysis connects without any doubts both TSs, with respective MCs and respective products.

In the second part of our research, we decided to perform a similar study regarding to the **1a**+**2a** process for the simulated presence of polar solvent—nitromethane. It was found, that both, the nature of energy profiles, as well as the quantitative description of all critical points, are close to results obtained for the simulated presence of toluene. Parallel, we detected two alternative channels of the addition reactions between considered reagents, which are not available in the toluene solution (paths **C** and **D**) (Scheme 5). In both cases, the first stage of the reaction is—similarly as in the case of 32CAs process—the formation of pre-reaction **MC** complexes. Their nature is close, to observed for cycloaddition reactions, but their further transformations proceed via different mechanistic scheme. In particular, conversion of mentioned MCs, leads directly to transition states **TSC** and **TCD**, respectively. Within these TSs, the distance between reaction centers C5-N1 are reduced to values, which can be considered as the stage of the formation of new sigma-bond. At the same time, the distances C3-C4 are characterized by values which are beyond of the typical range for formed sigma-bonds in transition states. Both localized TSs exhibit evidently polar nature, which is confirmed by analysis of GEDT values (Tables 4 and 5). The further

conversion of **TSC** and **TSD** leads directly for acyclic adducts **Z1** and **Z2**, respectively. This was confirmed by IRC analysis. Optimized adducts exhibit zwitterionic nature, which is evidently right due to GEDT values (GEDT > 1e). The direct transformation of these zwitterions into cycloadduct is however impossible, as the consequence of their conformation. The theoretically possible transformations from **Z1** or **Z2** to pyrazoline systems must proceed via dissociation in to individual reagents, and, in next step, via 32CA processes described above. Only, transformation between **Z1** and **Z2** zwitterions are possible, according to the simple rotation around C5-N1 bond.

Lastly, we examined the influence of the substituents' nature into reaction course. It was found that, the molecular reaction mechanism in all cases is close to observed for 32CAs involving diarylnitrylimine **1a** and ACN **2a**. In particular, in any case the stepwise zwitterionic mechanism was not detected. Only, the qualitative description of energy profile as well as key structures were changing in some range.

Table 2. DFT kinetic and thermodynamic parameters for the 32Cas of diarylnitrylimines **1a–e** and ACNs **2a–c** in toluene (ΔH, ΔG are in kcal/mol; ΔS are in cal/mol·K).

Reaction	Path	Transition	ΔH	ΔG	ΔS
1a+2a	**A**	**1a+2a→MCA**	−12.1	1.4	−45.2
		1a+2a→TSA	−6.1	8.4	−48.6
		1a+2a→3aa	−56.5	−40.0	−55.4
	B	**1a+2a→MCB**	−11.2	2.2	−45.0
		1a+2a→TSB	−7.2	8.3	−52.1
		1a+2a→4aa	−58.5	−42.3	−54.3
1b+2a	**A**	**1b+2a→MCA**	−13.1	0.4	−45.3
		1b+2a→TSA	−6.9	7.8	−49.5
		1b+2a→3ba	−56.6	−41.5	−50.7
	B	**1b+2a→MCB**	−13.1	0.4	−45.3
		1b+2a→TSB	−9.6	6.1	−52.8
		1b+2a→4ba	−59.0	−42.9	−54.0
1c+2a	**A**	**1c+2a→MCA**	−7.8	4.8	−42.5
		1c+2a→TSA	−2.5	12.8	−51.2
		1c+2a→3ca	−53.8	−37.2	−55.7
	B	**1c+2a→MCB**	−7.8	4.8	−42.5
		1c+2a→TSB	−2.6	13.1	−52.5
		1c+2a→4ca	−55.0	−38.3	−55.9
1d+2a	**A**	**1d+2a→MCA**	−10.2	4.8	−50.2
		1d+2a→TSA	−8.2	7.5	−52.9
		1d+2a→3da	−54.7	−36.7	−60.6
	B	**1d+2a→MCB**	−10.2	4.8	−50.2
		1d+2a→TSB	−6.7	9.9	−55.5
		1d+2a→4da	−56.9	−39.1	−59.9
1e+2a	**A**	**1e+2a→MCA**	−11.7	3.5	−51.1
		1e+2a→TSA	−3.0	13.0	−53.8
		1e+2a→3ea	−57.1	−40.2	−56.7
	B	**1e+2a→MCB**	−11.7	3.5	−51.1
		1e+2a→TSB	−5.9	10.5	−55.2
		1e+2a→4ea	−58.6	−41.1	−58.7
1a+2b	**A**	**1a+2b→MCA**	−12.9	0.4	−44.4
		1a+2b→TSA	−2.3	13.0	−51.5
		1a+2b→3ab	−52.8	−36.3	−55.5
	B	**1a+2b→MCB**	−15.4	−0.6	−49.5
		1a+2b→TSB	−3.9	11.6	−52.2
		1a+2b→4ab	−54.3	−37.3	−57.1
1a+2c	**A**	**1a+2c→MCA**	−17.0	−1.6	−51.5
		1a+2c→TSA	−8.8	5.8	−49.0
		1a+2c→3ac	−58.7	−42.9	−53.0
	B	**1a+2c→MCB**	−17.0	−1.6	−51.5
		1a+2c→TSB	−9.7	5.7	−51.4
		1a+2c→4ac	−61.4	−42.6	−63.2

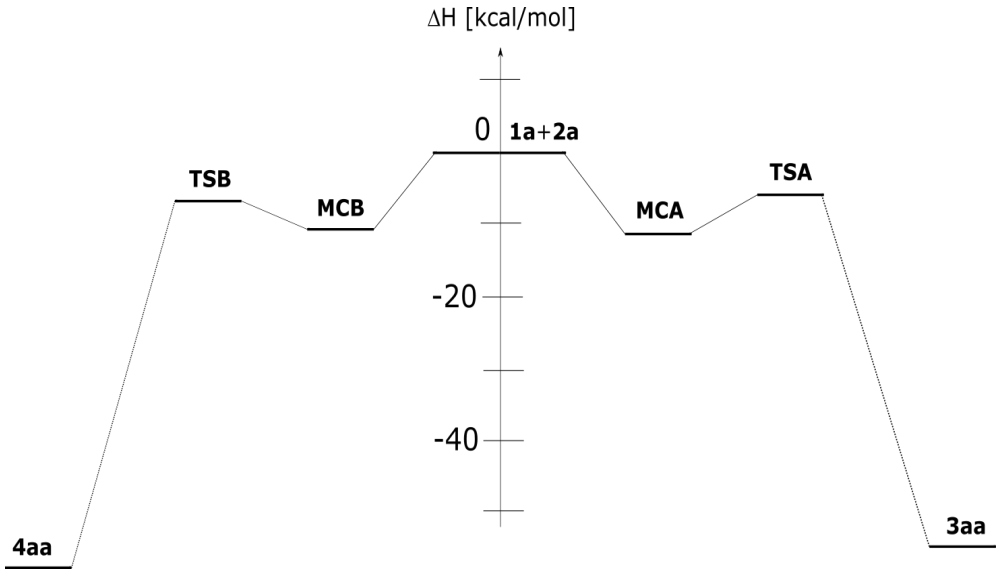

Figure 2. Enthalpy profile for the 32CA between diarylnitrylimine **1a** and can **2a** in toluene solution according to the DFT computational study.

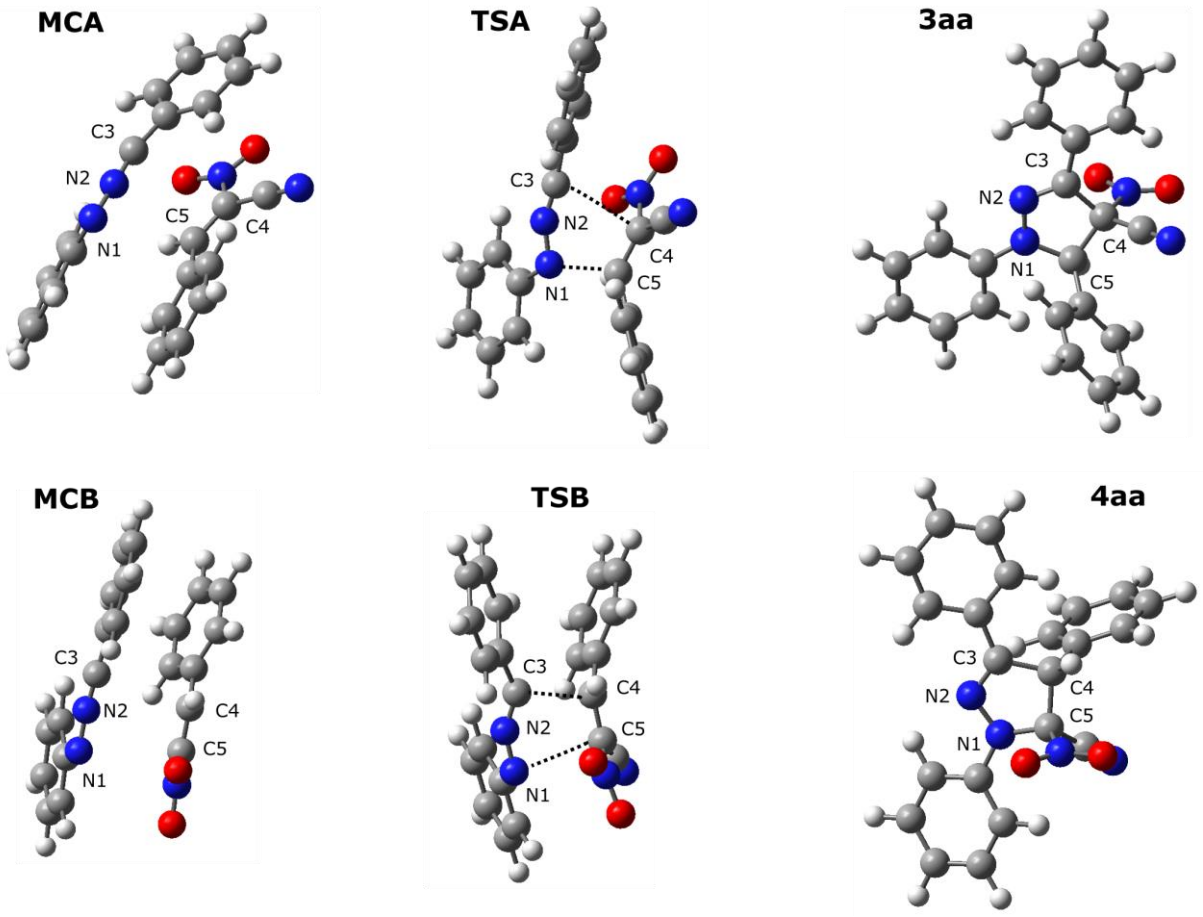

Figure 3. Views of key structures for the 32CA between diarylnitrylimine **1a** acanACN **2a** in toluene solution according to the DFT computational study.

Table 3. DFT kinetic and thermodynamic parameters for the 32Cas of diphenylnitrylimine **1a** and (E)-2-phenyl-1-cyano-1-nitroethenes **2a** in nitromethane (ΔH, ΔG are in kcal/mol; ΔS are in cal/mol·K).

Reaction	Path	Transition	ΔH	ΔG	ΔS
1a+2a	**A**	**1a+2a→MCA**	−10.9	1.6	−42.1
		1a+2a→TSA	−5.1	7.5	−42.4
		1a+2a→3aa	−53.3	−38.4	−50.0
	B	**1a+2a→MCB**	−10.9	1.6	−42.1
		1a+2a→TSB	−5.6	9.0	−48.9
		1a+2a→4aa	−55.3	−40.1	−50.9
	C	**1a+2a→MCC**	−12.0	−0.5	−38.4
		1a+2a→TSC	−3.9	9.1	−43.5
		1a+2a→Z1	−11.0	1.3	−41.4
		Z1→TS_{rot}	−11.1	3.5	−49.0
	D	**1a+2a→MCD**	−12.0	−0.5	−38.4
		1a+2a→TSD	−2.3	10.9	−44.2
		1a+2a→Z2	−10.5	2.4	−43.3

Table 4. Selected parameters for the key structures of the 32CAs of diarylnitrylimines **1a–e** and ACNs **2a–c**, in toluene, obtained from DFT calculations.

Reaction	Structure	Interatomic Distances [Å]					I_{C3-C4}	I_{C5-N1}	ΔI	GEDT [e]
		N1-N2	N2-C3	C3-C4	C4-C5	C5-N1				
1a+2a	**MCA**	1.262	1.161	3.629	1.345	4.034				0.00
	TSA	1.280	1.163	2.867	1.393	2.032	0.120	0.608	0.49	0.67
	3aa	1.335	1.284	1.525	1.566	1.460				
	MCB	1.260	1.160	3.044	1.343	3.047				0.00
	TSB	1.244	1.200	2.176	1.380	2.646	0.566	0.119	0.45	0.39
	4aa	1.379	1.278	1.517	1.561	1.406				
1b+2a	**MCA**	1.253	1.167	3.354	1.345	4.727				0.00
	TSA	1.277	1.162	2.904	1.391	2.065	0.094	0.584	0.49	0.62
	3ba	1.328	1.286	1.524	1.567	1.458				
	MCB	1.253	1.167	3.354	1.345	4.727				0.00
	TSB	1.240	1.200	2.267	1.374	2.714	0.507	0.062	0.45	0.34
	4ba	1.376	1.280	1.518	1.557	1.400				
1c+2a	**MCA**	1.253	1.162	4.200	1.344	3.658				0.00
	TSA	1.289	1.164	2.793	1.400	1.972	0.172	0.651	0.48	0.72
	3ca	1.343	1.281	1.528	1.564	1.462				
	MCB	1.253	1.162	4.200	1.344	3.658				0.00
	TSB	1.251	1.203	2.131	1.382	2.569	0.595	0.182	0.41	0.31
	4ca	1.383	1.278	1.517	1.562	1.413				
1d+2a	**MCA**	1.267	1.160	3.040	1.343	2.965				0.00
	TSA	1.284	1.165	2.937	1.386	2.109	0.077	0.554	0.48	0.58
	3da	1.344	1.282	1.528	1.564	1.459				
	MCB	1.267	1.160	3.040	1.343	2.965				0.00
	TSB	1.246	1.205	2.213	1.377	2.605	0.542	0.144	0.40	0.30
	4da	1.386	1.280	1.518	1.559	1.404				
1e+2a	**MCA**	1.246	1.168	3.355	1.342	3.187				0.00
	TSA	1.278	1.165	2.745	1.399	1.990	0.198	0.639	0.44	0.67
	3ea	1.325	1.287	1.524	1.564	1.462				
	MCB	1.246	1.168	3.355	1.342	3.187				0.00
	TSB	1.239	1.201	2.158	1.381	2.683	0.577	0.098	0.48	0.43
	4ea	1.370	1.278	1.516	1.563	1.411				
1a+2b	**MCA**	1.264	1.159	3.705	1.358	4.033				0.00
	TSA	1.283	1.161	2.871	1.405	1.982	0.116	0.644	0.53	0.69
	3ab	1.334	1.284	1.523	1.568	1.461				
	MCB	1.260	1.159	4.983	1.354	4.679				0.00
	TSB	1.243	1.202	2.143	1.387	2.650	0.587	0.115	0.47	0.38
	4ab	1.380	1.279	1.517	1.562	1.406				
1a+2c	**MCA**	1.266	1.157	4.178	1.342	3.512				0.00
	TSA	1.281	1.162	2.874	1.389	2.045	0.118	0.596	0.48	0.67
	3ac	1.337	1.283	1.527	1.564	1.456				
	MCB	1.266	1.157	4.178	1.342	3.512				0.00
	TSB	1.244	1.200	2.216	1.375	2.619	0.540	0.138	0.40	0.38
	4ac	1.378	1.278	1.517	1.560	1.406				

Table 5. Selected parameters for the key structures of the 32CAs of diarylnitrylimines **1a–e** and ACNs **2a–c**, in nitromethane, obtained from DFT calculations.

Reaction	Structure	Interatomic Distances [Å]					I_{C3-C4}	I_{C5-N1}	ΔI	GEDT [e]
		N1-N2	N2-C3	C3-C4	C4-C5	C5-N1				
1a+2a	**MCA**	1.269	1.158	3.787	1.346	3.576				0.00
	TSA	1.280	1.160	2.938	1.389	2.096	0.072	0.566	0.49	0.59
	3aa	1.333	1.284	1.524	1.566	1.461				
	MCB	1.269	1.158	3.205	1.346	3.221				0.00
	TSB	1.242	1.198	2.179	1.383	2.704	0.564	0.075	0.49	0.43
	4aa	1.381	1.278	1.517	1.561	1.404				
	MCC	1.270	1.157	5.700	1.347	4.125				0.00
	TSC	1.290	1.155	4.699	1.393	2.062		0.65		0.60
	Z1	1.308	1.151	4.628	1.482	1.529				1.05
	MCD	1.270	1.157	5.700	1.347	4.125				0.00
	TSD	1.291	1.152	4.290	1.399	2.042		0.65		0.48
	Z2	1.296	1.150	4.410	1.487	1.515				1.12
	TS rot	1.294	1.151	4.613	1.483	1.511				1.21

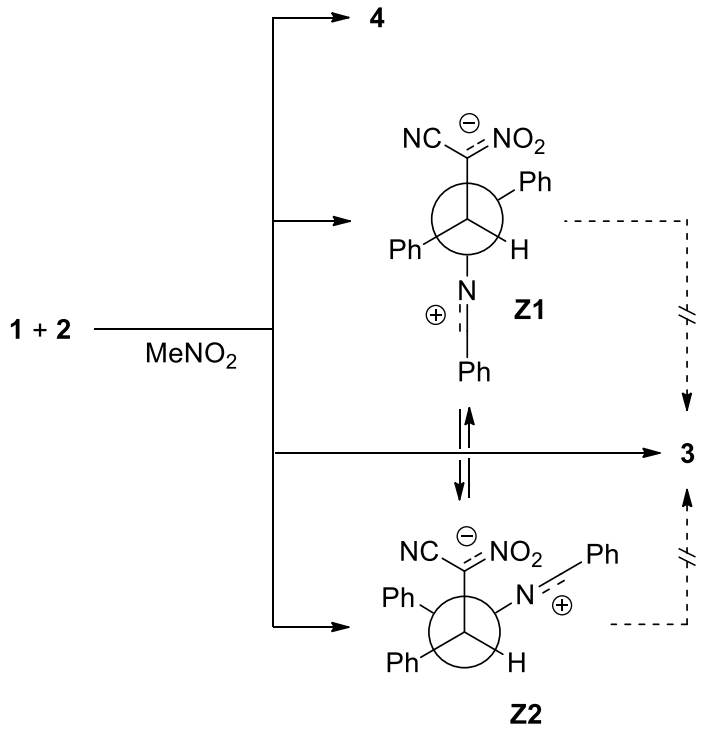

Scheme 5. The formation and transformations of zwitterionic intermediates derived via reactions between diarylnitrylimine **1a** and ACN **2a**.

3.3. BET Analysis of the 32CA between C,N-diphenylnitrylimine 1a and (E)-2-phenyl-1-cyano-1-nitroethene 2a

In order to carefully investigate the bonding changes occurring in the 32CA of the **1a** and **2a**, we decided to conduct a BET analysis. Scheme 6 represents the molecular mechanism by Lewis-like structures resulted from the ELF topological analysis. The most significant ELF basin populations together with attractor positions for a reaction leading to 4aa are gathered in Table 6 and Figure 4.

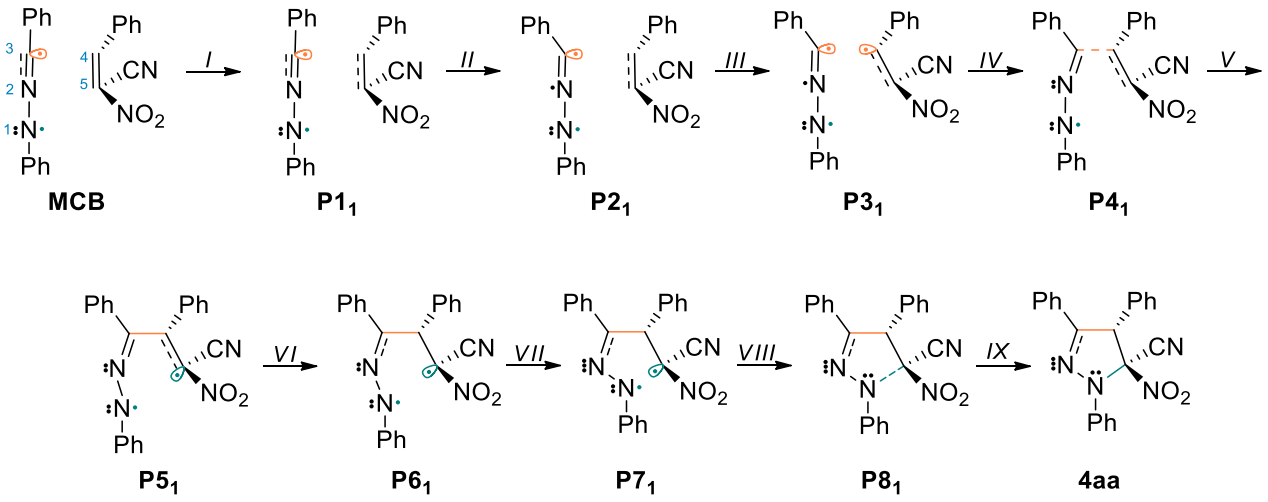

Scheme 6. The proposed molecular mechanism of the 32CA reaction between **1a** and **2a**.

Table 6. BET analysis results for the 32CA reaction of the **1a** with **2a**. The table also lists the structures **1a**, **2a**, **MCB**, **TSB** and **4aa**.

Points	1a	2a	MCB	P1$_1$	P2$_1$	P3$_1$	P4$_1$	P5$_1$	P6$_1$	P7$_1$	P8$_1$	4aa	TSB
Phases			*I*	*I–II*	*II–III*	*III–IV*	*IV–V*	*V–VI*	*VI–VII*	*VII–VIII*	*VIII–IX*	*IX*	
d(C3−C4)			2.803	2.634	2.240	2.079	2.014	1.884	1.605	1.548	1.541	1.521	2.176
d(C5−N1)			2.871	2.811	2.664	2.619	2.600	2.562	2.335	1.841	1.750	1.473	2.646
ΔE			0.0	1.9	3.6	3.3	2.6	0.2	−10.0	−27.7	−39.4	−47.3	4.0
V(N1,N2)	2.26		2.19	2.25	2.09	2.08	2.09	2.06	1.94	1.69	1.61	1.55	2.09
V(N1)	3.45		3.43	3.32	3.10	2.96	2.93	2.83	2.76	2.44	2.34	2.09	3.02
V(N2,C3)	2.72		2.76	2.67	2.27	2.14	2.10	2.00	3.17	3.23	3.18	3.17	2.20
V′(N2,C3)	2.17		2.39	2.35	1.81	1.53	1.51	1.50					1.69
V(C3)	0.99		0.70	0.85	1.16	1.26							1.20
V(N2)					0.94	1.42	1.54	1.74	2.37	2.68	2.74	2.78	1.17
V(C4,C5)		1.79	1.93	3.45	3.42	3.28	3.25	2.84	2.35	2.13	2.06	2.00	3.53
V′(C4,C5)		1.74	1.58										
V(C4)						0.16							
V(C3,C4)							1.41	1.62	1.90	1.94	1.95	1.98	
V(C5)								0.41	0.60	0.75			
V′(N1)										0.48			
V(C5,N1)											1.35	1.71	

[a] Relative to the first point of the IRC, **MCB**. Distances are given in angstroms, Å, and electron populations in average number of electrons, e, relative energies in kcal·mol^{-1}.

The bonding changes along this 32CA between C,N- diphenylnitrylimine **1a** and **2a** are characterized by nine different topological phases (Table 4). The ELF picture of the first structure **MCB** is very similar to those of the divided reagents. *Phase II* begins at **P1$_1$**, where it can be observed that the V(C4,C5) and V′(C4,C5) disynaptic basins current in previous **MCB** point, have combined into one new V(C4,C5) disynaptic basin with initial population 3.45 e. Along *Phase III*, which begins at **P2$_1$**, the new V(N2) monosynaptic basin is created with population of 0.94 e. Creation of this monosynaptic basin is related to depopulation of V(N1,N2), V(N2,C3) and V′(N2,C3) disynaptic basins and the growth of the population of V(C3) monosynaptic basin. At this point, we found the TS structure of the 32CA between **1a** and **2a** (**TSB**, d(C3-C4) = 2.176 Å and d(C5-N1) = 2.646 Å). *Phase IV* initiates at the structure **P3$_1$**, where can be noticed the creation of a V(C4) monosynaptic basin with 0.16 e, which is connected with depopulation of V(C4,C5) disynaptic basin. Creation of this monosynaptic basin is associated with formation a *pseudoradical* [46] center at C4 carbon atom (Figure 4).

Along *Phase V*, which begins at **P4$_1$**, we noticed that *pseudoradical* centers located on C3 and C4 atoms combined into C3-C4 bonding area with an starting value of 1.41 e. The electron density changes mean that creation of the C3-C4 bond starts with a distance d(C3,C4) = 2.014 Å, by divvying the non-bonding electron densities of the two C3 and C4 centers. *Phase VI*, starts at **P5$_1$**, and is related to formation a new *pseudoradical* center at C5 carbon atom with value of 0.41 e (Figure 4 and Table 6). Formation of a new V(C5) monosynaptic basin causes depopulation of V(C4,C5) disynaptic basin. In *Phase VII*, the V(N2,C3) and V′(N2,C3) disynaptic basins, have merged and a new V(N2,C3) disynaptic basin was created with 3.17 e. This shift is related to disruption of the N2-C3 bond and formation a partial double bond (Scheme 6). At **P7$_1$** begins *Phase VIII*, which is associated with creation a V′(N2) monosynaptic basin with starting value of 0.48 e. This shift is caused by division of V(N1) monosynaptic basin, present in **P6$_1$**, for two new V(N1) and V′(N1) monosynaptic basins and depopulation of V(N1,N2) disynaptic basin. Subsequently we observed in the last *Phase IX*, which is located between **P8$_1$** and **4aa** (Table 6). In this phase, the creation of the second C5-N1 bond follows through the connection of the non-bonding electron densities of the two V(C5) and V(N1) monosynaptic basins. The C5-N1 bond was formed with starting distance of d(C5,N1) = 1.750 Å.

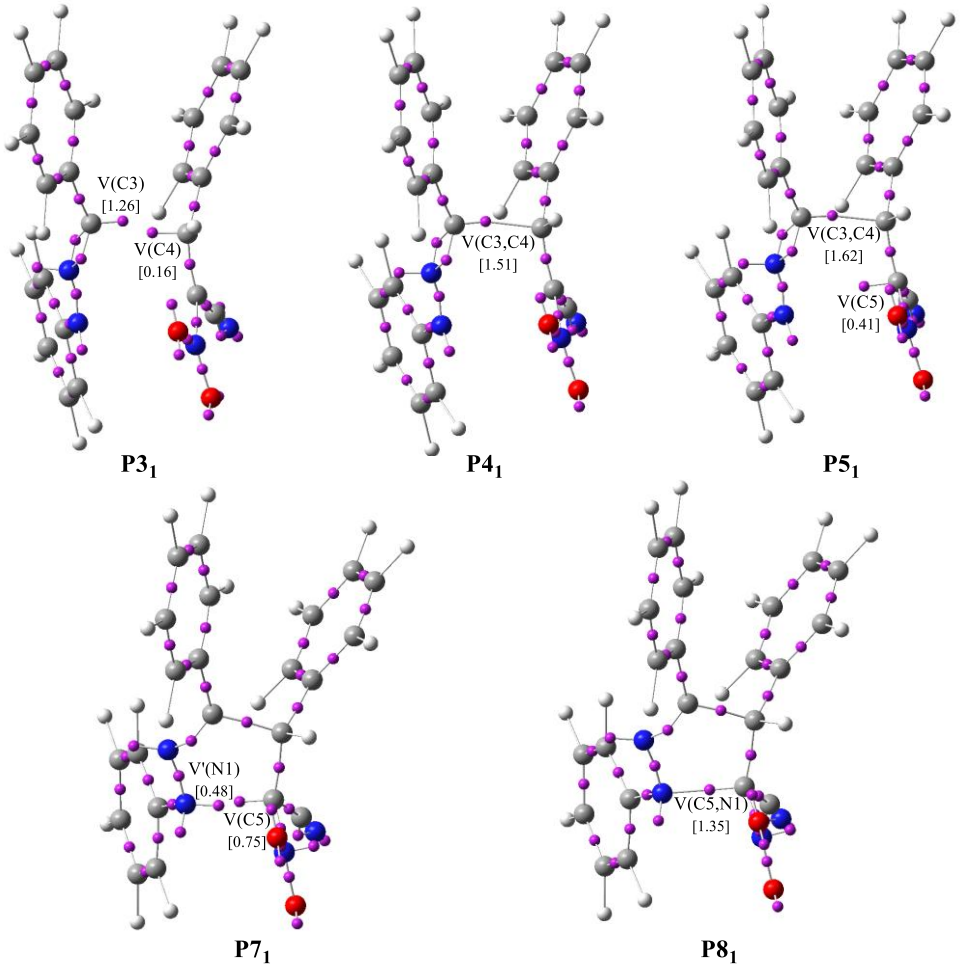

Figure 4. The main ELF valence basin populations for the points P3$_1$–P5$_1$, P7$_1$ and P8$_1$ participating in the 32CA reaction of the **1a** and **2a**.

On the grounds of the BET study, we gather that: (i) the 32CA reaction between C,N-diphenylnitrylimine **1a** and (E)-2-phenyl-1-cyano-1-nitroethene **2a** can be depicted by nine topologically various phases; (ii) the activation energy of this reaction, 4.0 kcal·mol^{-1}, is related to the formation of C4 *pseudoradical* center and lone pair at N2 nitrogen atom;

(iii) creation of first C3-C4 bond follows in *Phase V* by way of merging two C3 and C *pseudoradical* centers; (iv) creation of the C5-N1 bond occurs in the last *Phase IX* by merging the C5 *pseudoradical* center and N1 non-bonding lone pair; (v) it is worth nothing that when the C5-N1 bond begins to form, the first bond is fully formed. According to that, we can conclude that the 32CA of the **1a** and **2a** proceeds according to *one-step two-stage* mechanism.

3.4. BET Study of the Creation of Acyclic Adduct Z1

We also decided to analyze the bonding changes along the formation acyclic adduct **Z1** by doing the BET analysis. The most significant ELF basin populations and attractor positions for structures participating in the studied reaction are collected in Table 7 and Figure 5.

Table 7. BET analysis results for the formation of acyclic adduct **Z1**. The table also lists the structures **1a**, **2a**, **MCC**, **TSC** and **Z1**.

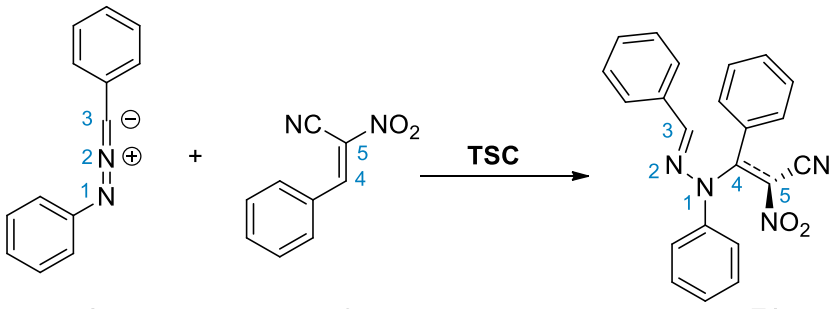

1a **2a** **Z1**

Points	**1a**	**2a**	**MCC**	**P1$_2$**	**P2$_2$**	**P3$_2$**	**P4$_2$**	**P5$_2$**	**P6$_2$**	**P7$_2$**	**Z1**	**TSC**
Phases			*I*	*I–II*	*II–III*	*III–IV*	*IV–V*	*V–VI*	*VI–VII*	*VII–VIII*	*VIII*	
d(C4−N1)			3.074	2.775	2.381	2.242	1.937	1.875	1.844	1.753	1.544	2.062
ΔE			0.0	2.3	5.4	7.6	6.8	5.1	3.7	2.2	1.0	8.1
V(N1,N2)	2.26		2.15	2.09	2.10	2.06	1.97	1.93	1.91	1.87	1.75	2.00
V(N1)	3.45		3.49	3.51	3.41	3.47	3.48	2.26	2.20	2.09	1.92	3.40
V(N2,C3)	2.72		2.97	3.20	3.81	5.87	5.83	5.85	5.86	4.98	4.30	5.84
V′(N2,C3)	2.17		2.36	2.13	2.00							
V(C3)	0.99		0.45	0.27								
V(C4,C5)		1.79	1.89	3.49	3.51	3.53	2.95	2.54	2.31	2.28	2.04	3.52
V′(C4,C5)		1.74	1.66									
V(C5)							0.56	0.64	0.65	0.73	0.74	
V(C4,N1)								1.31	1.41	1.52	1.77	
V′(C5)									0.37	0.43	0.57	
V(N2)										0.89	1.64	

[a] Relative to the first point of the IRC, **MCC**. Distances are given in angstroms, Å, and electron populations in average number of electrons, e, relative energies in kcal·mol^{-1}.

The bonding changes along the formation of acyclic adduct **Z1** are described by eight various phases (Table 7). The first point of the IRC is the molecular complex **MCC**, which presents ELF picture of separated reagents. We observed that the V(N1) monosynaptic and V(N2,C3), V′(N2,C3) and V(C4,C5) disynaptic basins show a slight larger ELF valence basin populations than those shown in the substrates. In turn, in the event of V(N1,N2) and V′(C4,C5) disynaptic and V(C3) monosynaptic basins, we observed the lower values of the ELF basin populations. *Phase II* begins at structure **P1$_2$**. In this area, the two V(C4,C5) and V′(C4,C5) disynaptic basins merged into one new V(C4,C5) disynaptic basin with starting population of 3.49 e. This topological shift is connected with break of C4-C5 bond in (E)-2-phenyl-1-cyano-1-nitroethene **2a**. Along *Phase III*, the C3 monosynaptic basin disappear and we observed the increase in the population of V(N2,C3) disynaptic basin to about 3.81 e. Along *Phase IV*, the V(N2,C3) and the V′(N2,C3) disynaptic basins merged into one original

V(N2,C3) disynaptic basin integrating 5.87 e. At $\mathbf{P3_2}$, we notice the TS of the formation of adduct **Z1** (**TSC**, d(C4-N1) = 2.062 Å). *Phase V* begins at $\mathbf{P4_2}$ and is related to create a V(C5) monosynaptic basin integrating 0.56 e. This is connected with a creation of *pseudoradical* center at C5 carbon atom and depopulation of V(C4,C5) disynaptic basin. In *Phase VI*, we observed the formation a new V(C4,N1) disynaptic basin with population of 1.31 e, created by depopulation of V(N1) monosynaptic and V(C4,C5) disynaptic basins. This topological change is associated with formation of the C4-N1 single bond (Figure 5). The next *Phase VII* begins at $\mathbf{P6_2}$ and is associated with creation of a second V′(C5) monosynaptic basin with population of 0.37 e. Forming of *pseudoradical* center at C5 carbon atom is associated with decrease the population of V(C4,C5) disynaptic basin. The final *Phase VIII*, placed between $\mathbf{P7_2}$ and **Z1** is related to formation a V(N2) monosynaptic basin through the depopulation of V(N2,C3) disynaptic basin.

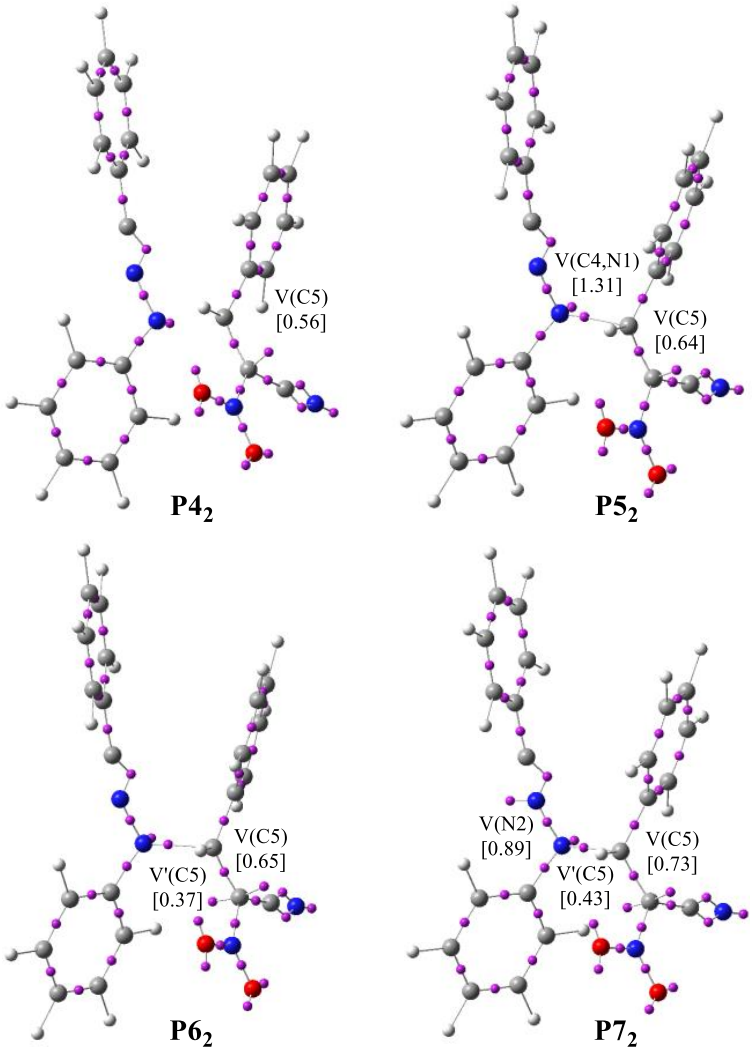

Figure 5. The main ELF valence basin populations for the points $\mathbf{P4_2}$–$\mathbf{P7_2}$ participating in the formation of **Z1**.

On the basis of BET study, we may say that: (i) the molecular mechanism of the formation of acyclic adduct **Z1** can be featured by eight various phases; (ii) the activation energy of this reaction, 8.1 kcal·mol^{-1}, is mostly related to breaking of the N2-C3 double bond and formation of C5 *pseudoradical* center; (iii) formation of C4-N1 single bond takes place in *Phase VI* by the depopulation of V(N1) monosynaptic and V(C4,C5) disynaptic basins.

4. Conclusions

The DFT computational study shows, that despite of high electrophilic nature of nitroalkenes, the [3+2] cycloaddition reactions between diarylnitrylimines and 2-aryl-1-cyano-1-nitroethenes proceed via single-step mechanism. In a polar nitromethane solution, the cycloaddition process can however compete, with the formation of zwitterionic structures characterized by "extended" conformations. These intermediates cannot be cyclized in to heterocyclic systems via simple one-step reactions, because the key reaction sites are localized on too long relative distance. Their conversion into pyrazoline systems is possible only via the stage of dissociation into individual reagents, and subsequently, one-step cycloaddition.

The topological analysis of the bonding changes associated with 32CA reaction between C,N-diphenylnitrylimine **1a** and (E)-2-phenyl-1-cyano-1-nitroethene **2a**, can be described by nine topologically different phases. Formation of the first C-C single bond follows by merging of two *pseudoradical* centers. In turn, the second C-N bond is formed in the last phase of the reaction when the first bond is fully formed. According to that, we can conclude that the 32CA of the **1a** and **2a** progress according to *one-step two-stage* mechanism.

Author Contributions: Conceptualization, R.J.; methodology, K.Z., P.W., K.K., A.K.-Z. and A.Ł.-K.; software, R.J., K.Z., P.W., K.K., A.K.-Z. and A.Ł.-K.; formal analysis, R.J., K.Z., K.K. and A.K.-Z.; investigation, R.J., K.Z., P.W., K.K., A.K.-Z. and A.Ł.-K.; writing—original draft preparation, R.J., K.Z., K.K. and A.K.-Z.; writing—review and editing, A.F. and A.O.; visualization, R.J., A.F., A.O., K.K. and A.K.-Z.; supervision, R.J., K.Z., K.K. and A.K.-Z. All authors have read and agreed to the published version of the manuscript.

Funding: This research received no external funding.

Institutional Review Board Statement: Not applicable.

Informed Consent Statement: Not applicable.

Data Availability Statement: The data presented in this study are available on request from the corresponding author.

Conflicts of Interest: The authors declare no conflict of interest.

References

1. Ried, W.; Köhler, E. Reaktionen mit Nitro-acetonitril. *Lieb. Ann. Chem.* **1956**, *598*, 145–158. [CrossRef]
2. Kanishchev, M.I.; Korneeva, N.; Shevelev, S.A. Synthesis of 3-amino-5-benzylamino-4-nitropyrazole. *Bull. Acad. Sci. USSR* **1986**, *35*, 2145–2147. [CrossRef]
3. Boguszewska-Czubara, A.; Kula, K.; Wnorowski, A.; Biernasiuk, A.; Popiołek, Ł.; Miodowski, D.; Demchuk, O.M.; Jasiński, R. Novel functionalized β-nitrostyrenes: Promising candidates for new antibacterial drugs. *Saudi Pharm. J.* **2019**, *27*, 593–601. [CrossRef] [PubMed]
4. Jasiński, R.; Mirosław, B.; Demchuk, O.M.; Babyuk, D.; Łapczuk-Krygier, A. In the search for experimental and quantumchemical evidence for zwitterionic nature of (2E)-3-[4-(dimethylamino)phenyl]-2-nitroprop-2-enenitrile—An extreme example of donor–π–acceptor push–pull molecule. *J. Mol. Struct.* **2016**, *1108*, 689–697. [CrossRef]
5. Łapczuk-Krygier, A.; Ponikiewski, Ł.; Jasiński, R. The crystal structure of (1RS,4RS,5RS,6SR)-5-cyano-5-nitro-6-phenylbicyclo[2.2.1]hept-2-ene. *Crystallogr. Rep.* **2014**, *59*, 961–963. [CrossRef]
6. Łapczuk-Krygier, A.; Jasiński, R. New Endo-Nitro-Substituted Norbornene Derivatives and Stereoselective Method for Producing New Endo-Nitro-Substituted Norbornene Derivatives. Patent No. PL 231749, 13 March 2017.
7. Poos, G.I.; Kleis, J.; Wittekind, R.R.; Rosenau, J.D. Bicyclic Bases. III. Isomeric 2-Amino-3-phenylnorbornanes. *J. Org. Chem.* **1961**, *26*, 4898–4904. [CrossRef]
8. Żmigrodzka, M.; Dresler, E.; Hordyjewicz-Baran, Z.; Kulesza, R.; Jasiński, R. A unique example of noncatalyzed 32CAinvolving (2E)-3-aryl-2-nitroprop-2-enenitriles. *Chem. Heterocycl. Compd.* **2017**, *53*, 1161–1162. [CrossRef]
9. Jasiński, R.; Kula, K.; Kącka, A.; Mirosław, B. Unexpected course of reaction between (E)-2-aryl-1-cyano-1-nitroethenes and diazafluorene: Why is there no 1,3-dipolar cycloaddition? *Mon. Chem.* **2017**, *148*, 909–915. [CrossRef]
10. Woliński, P.; Kącka-Zych, A.; Demchuk, O.M.; Łapczuk-Krygier, A.; Mirosław, B.; Jasiński, R. Clean and molecularly programmable protocol for preparation of bis-heterobiarylic systems via a domino pseudocyclic reaction as a valuable alternative for TM-catalyzed cross-couplings. *J. Clean. Prod.* **2020**, *275*, 122086. [CrossRef]
11. Parr, R.G.; Szentpaly, L.V.; Liu, S. Electrophilicity Index. *J. Am. Chem. Soc.* **1999**, *121*, 1922–1924. [CrossRef]

12. Domingo, L.R.; Ríos-Gutiérrez, M.; Pérez, P. Applications of the Conceptual Density Functional Theory Indices to Organic Chemistry Reactivity. *Molecules* **2016**, *21*, 748. [CrossRef] [PubMed]
13. Pérez, P.; Domingo, L.R.; Duque-Noreña, M.; Chamorro, E. A condensed-to-atom nucleophilicity index. An application to the director effects on the electrophilic aromatic substitutions. *J. Mol. Struct.* **2009**, *895*, 86–91. [CrossRef]
14. Greelings, P.; De Proft, F.; Langenaeker, W. Conceptual Density Functional Theory. *Chem. Rev.* **2003**, *103*, 1793–1874. [CrossRef] [PubMed]
15. Zawadzińska, K.; Kula, K. Application of ß-phosphorylated nitroethenes in [3+2] cycloaddition reactions involving benzonitrile N-oxide in the light of DFT computational study. *Organics* **2021**, *2*, 26–37. [CrossRef]
16. Pérez, P.; Domingo, L.R.; Aurell, M.J.; Contreras, R. Quantitative characterization of the global electrophilicity pattern of some reagents involved in 1.3-dipolar cycloaddition reactions. *Tetrahedron* **2003**, *59*, 3117–3125. [CrossRef]
17. Domingo, L.R.; Pérez, P.; Saez, J.A. Understanding the local reactivity in polar organic reactions through electrophilic and nucleophilic Parr functions. *RSC Adv.* **2013**, *3*, 1486–1494. [CrossRef]
18. Frisch, M.J.; Trucks, G.W.; Schlegel, H.B.; Scuseria, G.E.; Robb, M.A.; Cheeseman, J.R.; Scalmani, G.; Barone, V.; Petersson, G.A.; Fox, D.J.; et al. (Eds.) *Gaussian 16*; Revision, A.03; Gaussian, Inc.: Wallingford, CT, USA, 2016.
19. Barone, V.; Cossi, M.; Tomasi, J. Geometry Optimization of Molecular Structures in Solution by the Polarizable Continuum Model. *J. Comput. Chem.* **1998**, *19*, 404–417. [CrossRef]
20. Domingo, L.R. A new C–C bond formation model based on the quantum chemical topology of electron density. *RSC Adv.* **2014**, *4*, 32415–32428. [CrossRef]
21. Jasiński, R. A stepwise, zwitterionic mechanism for the 1,3-dipolar cycloaddition between (Z)-C-4-methoxyphenyl-N-phenylnitrone and gem-chloronitroethene catalysed by 1-butyl-3-methylimidazolium ionic liquid cations. *Tetrahedron Lett.* **2015**, *56*, 532–535. [CrossRef]
22. Silvi, B.; Savin, A. Classification of chemical bonds based on topological analysis of electron localization functions. *Nature* **1994**, *371*, 683–686. [CrossRef]
23. Savin, A.; Silvi, B.; Colonna, F. Topological Analysis of the Electron Localization Function Applied to Delocalized Bonds. *Can. J. Chem.* **1996**, *74*, 1088–1096. [CrossRef]
24. Becke, A.D.; Edgecombe, K.E. A simple measure of electron localization in atomic and molecular systems. *J. Chem. Phys.* **1990**, *92*, 5397–5403. [CrossRef]
25. Krokidis, K.; Noury, S.; Silvi, B. Characterization of Elementary Chemical Processes by Catastrophe Theory. *J. Phys. Chem. A* **1997**, *101*, 7277–7281. [CrossRef]
26. Noury, S.; Krokidis, K.; Fuster, F.; Silvi, B. Computational tools for the electron localization function topological analysis. *Comput. Chem.* **1999**, *23*, 597–604. [CrossRef]
27. Mirosław, B.; Babyuk, D.; Łapczuk-Krygier, A.; Kącka-Zych, A.; Demchuk, O.M.; Jasiński, R. Regiospecific formation of the nitromethyl-substituted 3-phenyl-4,5-dihydroisoxazole via [3+2] cycloaddition. *Chem. Mon.* **2018**, *149*, 1877–1884. [CrossRef]
28. Kula, K.; Dobosz, J.; Jasiński, R.; Kącka-Zych, A.; Łapczuk-Krygier, A.; Mirosław, B.; Demchuk, O.M. [3+2] Cycloaddition of diaryldiazomethanes with (E)-3,3,3-trichloro-1-nitroprop-1-ene: An experimental, theoretical and structural study. *J. Mol. Struct.* **2020**, *1203*, 127473. [CrossRef]
29. Kącka-Zych, A.; Domingo, L.R.; Ríos-Gutiérrez, M.; Jasiński, R. Understanding the mechanism of the decomposition reaction of nitroethyl benzoate through the Molecular Electron Density Theory. *Theor. Chem. Acc.* **2017**, *136*, 129. [CrossRef]
30. Kącka-Zych, A.; Jasiński, R. Unexpected molecular mechanism of trimethylsilyl bromide elimination from 2-(trimethylsilyloxy)-3-bromo-3-methyl-isoxazolidines. *Theor. Chem. Acc.* **2019**, *138*, 81. [CrossRef]
31. Woliński, P.; Kącka-Zych, A.; Dziuk, B.; Ejsmont, K.; Łapczuk-Krygier, A.; Dresler, E. The structural aspects of the transformation of 3-nitroisoxazoline-2-oxide to 1-aza-2,8-dioxabicyclo[3.3.0]octane derivatives: Experimental and MEDT theoretical study. *J. Mol. Struct.* **2019**, *1192*, 27–34. [CrossRef]
32. Kącka, A.; Jasiński, R. A dramatic change of kinetic conditions and molecular mechanism of decomposition processes of nitroalkyl carboxylates catalyzed by ethylammonium cations. *Comput. Theor. Chem.* **2017**, *1104*, 37–42. [CrossRef]
33. Kącka-Zych, A. Participation of Phosphorylated Analogues of Nitroethene in Diels–Alder Reactions with Anthracene: A Molecular Electron Density Theory Study and Mechanistic Aspect. *Organics* **2020**, *1*, 36–48. [CrossRef]
34. Kącka-Zych, A. The Molecular Mechanism of the Formation of Four-Membered Cyclic Nitronates and Their Retro (3+2) Cycloaddition: A DFT Mechanistic Study. *Molecules* **2021**, *26*, 4786. [CrossRef] [PubMed]
35. Domingo, L.R. Molecular Electron Density Theory: A modern view of reactivity in organic chemistry. *Molecules* **2016**, *21*, e1319. [CrossRef]
36. Chattaraj, P.K.; Sarkar, U.; Roy, D.R. Electrophilicity index. *J. Am. Chem. Soc.* **1999**, *121*, 1922–1924. [CrossRef]
37. Kula, K.; Zawadzinska, K. Local nucleophile-electrophile interactions in [3+2] cycloaddition reactions between benzonitrile N-oxide and selected conjugated nitroalkenes in the light of MEDT computational study. *Curr. Chem. Lett.* **2021**, *10*, 9–16. [CrossRef]
38. Domingo, L.R.; Kula, K.; Ríos-Gutiérrez, M. Unveiling the reactivity of cyclic azomethine ylides in [3+2] cycloaddition reactions within the Molecular Electron Density Theory. *Eur. J. Org. Chem.* **2020**, 5938–5948. [CrossRef]
39. Mlostoń, G.; Kula, K.; Jasiński, R. A DFT Study on the Molecular Mechanism of Additions of Electrophilic and Nucleophilic Carbenes to Non-Enolizable Cycloaliphatic Thioketones. *Molecules* **2021**, *26*, 5562. [CrossRef]

40. Domingo, L.R.; Kula, K.; Ríos-Gutiérrez, M.; Jasiński, R. Understanding the Participation of Fluorinated Azomethine Ylides in Carbenoid-Type [3+2] Cycloaddition Reactions with Ynal Systems: A Molecular Electron Density Theory Study. *J. Org. Chem.* **2021**, *86*, 12644–12653. [CrossRef]
41. Domingo, L.R.; Ríos-Gutiérrez, M.; Pérez, P. A molecular electron density theory study of the participation of tetrazines in aza-Diels–Alder reactions. *RSC Adv.* **2020**, *10*, 15394–15405. [CrossRef]
42. Zawadzińska, K.; Ríos-Gutiérrez, M.; Kula, K.; Woliński, P.; Mirosław, B.; Krawczyk, T.; Jasiński, R. The Participation of 3,3,3-Trichloro-1-nitroprop-1-ene in the [3+2] Cycloaddition Reaction with Selected Nitrile N-Oxides in the Light of the Experimental and MEDT Quantum Chemical Study. *Molecules* **2021**, *26*, 6774. [CrossRef]
43. Mlostoń, G.; Jasiński, R.; Kula, K.; Heimgartner, H. A DFT Study on the Barton-Kellogg Reaction—The molecular mechanism of the formation of thiiranes in the reaction between diphenyldiazomethane and diaryl thioketones. *Eur. J. Org. Chem* **2020**, 176–182. [CrossRef]
44. Kula, K.; Kącka-Zych, A.; Łapczuk-Krygier, A.; Jasiński, R. Analysis of the possibility and molecular mechanism of carbon dioxide consumption in the Diels-Alder processes. *Pure Appl. Chem.* **2021**, *93*, 427–446. [CrossRef]
45. Domingo, L.R.; Ríos Gutiérrez, M.; Castellanos Soriano, J. Understanding the Origin of the Regioselectivity in Non-Polar [3+2] Cycloaddition Reactions through the Molecular Electron Density Theory. *Organics* **2020**, *1*, 19–35. [CrossRef]
46. Domingo, L.R.; Chamorro, E.; Pérez, P. Understanding the High Reactivity of the Azomethine Ylides in [3+2] Cycloaddition Reactions. *Lett. Org. Chem.* **2010**, *7*, 432–439. [CrossRef]